

## 3-Amino-2-hydroxyamides and related compounds as inhibitors of methionine aminopeptidase-2

George S. Sheppard,\* Jieyi Wang, Megumi Kawai, Nwe Y. BaMaung, Richard A. Craig, Scott A. Erickson, Linda Lynch, Jyoti Patel, Fan Yang, Xenia B. Searle, Pingping Lou, Chang Park, Ki H. Kim, Jack Henkin and Richard Lesniewski

*Abbott Laboratories, Global Pharmaceutical Research and Development, Cancer Research, 100 Abbott Park Road, Abbott Park, IL 60064, USA*

Received 9 October 2003; accepted 3 December 2003

**Abstract**—Substituted 3-amino-2-hydroxyamides and related hydroxyamides and acylhydrazines were identified as inhibitors of human methionine aminopeptidase-2 (MetAP2). Examination of substituents through parallel synthesis and iterative structure-based design allowed the identification of potent inhibitors with good selectivity against MetAP1. Diacylhydrazine **3t** (A-357300) was identified as an analogue displaying inhibition of methionine processing and cellular proliferation in human microvascular endothelial cells (HMVEC).

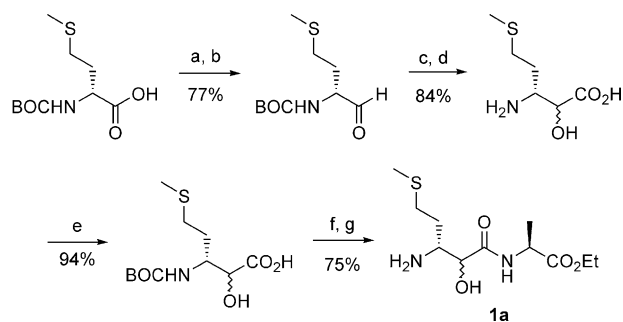
© 2003 Elsevier Ltd. All rights reserved.

Methionine aminopeptidases are metalloenzymes responsible for the removal of the N-terminal initiator methionine residue of nascent proteins. Humans have two forms of the enzyme, MetAP1 and MetAP2.<sup>1</sup> MetAP2 was demonstrated to be a molecular target of the antiangiogenic natural product fumagillin,<sup>2</sup> and its semisynthetic analogue TNP-470,<sup>3</sup> which irreversibly inactivate the enzyme by covalent modification of a histidine residue in the active site.<sup>4</sup> TNP-470 displays inhibitory activity in animal models of angiogenesis and tumor growth,<sup>5</sup> supporting the potential of MetAP2 inhibition as an approach to the treatment of cancer and other diseases with an angiogenic component.

As part of a program to discover reversible inhibitors of MetAP2, we examined several structural types reported in the literature as inhibitors of aminopeptidases, including 3-amino-2-hydroxyamides such as bestatin<sup>6</sup> and amastatin.<sup>7</sup> Contemporaneously with these investigations, others have examined related approaches to inhibition of MetAP1,<sup>8</sup> as well as MetAP2.<sup>9</sup> Analogues such as **1a** containing a methionine side chain at the 3-position provided reversible MetAP2 inhibitors (Table 1). As expected based on the bestatin analogy,<sup>10</sup>

the 2*S*,3*R* diastereomer was demonstrated to be the most active (data not shown). A series of substituted (2*SR*,3*R*)-3-amino-2-hydroxy-butanoic amides coupled to L-alanine ethyl ester were prepared from available D-amino acids using the route shown for **1a** in Scheme 1, and evaluated for inhibition of human MetAP2 and MetAP1 (Table 1) by a previously described method.<sup>11</sup>

As expected based on the published X-ray structure<sup>4</sup> and our own crystallography, the active site was able to accommodate sidechains larger than methionine, and required extended side-chains for good activity. Larger



**Scheme 1.** Reagents and conditions: (a) REDAL, toluene, 0–25 °C; (b) SO<sub>3</sub> pyridine, Et<sub>3</sub>N, DMSO; (c) NaHSO<sub>3</sub>, KCN, EtOAc/H<sub>2</sub>O; (d) 6M HCl, dioxane/H<sub>2</sub>O, reflux, 18 h; (e) BOC-ON, Et<sub>3</sub>N, dioxane/H<sub>2</sub>O; (f) EDCl, HOBT, NMM, L-AlaOEt; (g) HCl/dioxane.

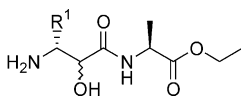
\* Corresponding author. Fax.: +1-847-935-5165; e-mail: george.sheppard@abbott.com

sidechains also showed a trend toward greater selectivity relative to MetAP1. Although we lack an X-ray structure of human MetAP1, this observation is consistent with a prediction of a smaller side chain binding area based on modeling of MetAP1, which lacks a 60 amino acid insertion forming part of the active site in MetAP2.

The initial series of analogues defined the approximate size and shape requirements of the enzyme active site. Investigation next turned to exploration of the amide group by parallel synthesis. Based on initial results, analogues of cyclohexylmethyl analogue **6a** were targeted for synthesis due to the potency and selectivity observed, as well as the ready availability of quantities of the intermediate BOC protected 3-amino-2-hydroxy acid with good diastereomeric purity at C2 due to selective crystallization of an intermediate. Parallel synthesis was carried out in 48 well reactors by activation of the acid as the HOAT ester using HATU (*O*-(7-azabenzotriazol-1-yl)-tetramethyluronium hexafluorophosphate) and DIEA in DMA for 10 min at ambient temperature, followed by amine addition and shaking at ambient temperature for 60–75 h. Following workup and solid phase extraction, the product amides were deprotected with 4N HCl in dioxane, and when necessary purified by RPHPLC. Over 500 compounds were characterized by <sup>1</sup>H NMR and MS and judged to have HPLC purity >90% prior to biological testing.

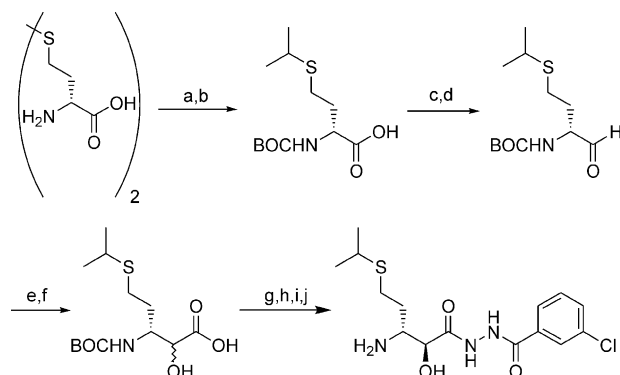
A subset of the testing results is shown in Table 2. A quick survey indicated both similarities and differences between our SAR and that reported for inhibition of aminopeptidase B by bestatin.<sup>10</sup> As in the bestatin case, the stereochemistry at C2 of alanine was not crucial (compounds **6b** and **6c**). However, in this case, presence of a carboxylate (**6d**) was detrimental to activity, in contrast to the aminopeptidase B case where the carboxyl is reported to be important for inhibition. Based on the reported substrate preference of MetAP2 for small amino acids such as alanine adjacent to the

**Table 1.** Inhibition of human methionine aminopeptidases



Compd	R <sup>1</sup>	MetAP2 IC <sub>50</sub> , μM <sup>a</sup>	MetAP1 IC <sub>50</sub> , μM <sup>a</sup>
<b>1a</b>	CH <sub>2</sub> CH <sub>2</sub> SCH <sub>3</sub>	5.7	63
<b>2a</b>	CH <sub>2</sub> CH <sub>2</sub> SCH <sub>2</sub> CH <sub>3</sub>	1.3	69
<b>3a</b>	CH <sub>2</sub> CH <sub>2</sub> SCH(CH <sub>3</sub> ) <sub>2</sub>	1.1	NT
<b>4a</b>	CH <sub>2</sub> CH <sub>2</sub> CH <sub>2</sub> CH <sub>3</sub>	8.0	100
<b>5a</b>	C <sub>6</sub> H <sub>11</sub>	12.5	NT
<b>6a</b>	CH <sub>2</sub> C <sub>6</sub> H <sub>11</sub>	0.6	84
<b>7a</b>	CH <sub>2</sub> CH <sub>2</sub> C <sub>6</sub> H <sub>5</sub>	0.46	101
<b>8a</b>	CH <sub>2</sub> CH <sub>2</sub> C <sub>6</sub> H <sub>11</sub>	0.59	137
<b>9a</b>	CH <sub>2</sub> SC(CH <sub>3</sub> ) <sub>3</sub>	1.6	14
<b>10a</b>	CH <sub>2</sub> SCH(CH <sub>3</sub> ) <sub>2</sub>	1.8	13
<b>11a</b>	CH <sub>2</sub> SCH <sub>2</sub> CH <sub>2</sub> CH <sub>3</sub>	1.4	57
<b>12a</b>	CH <sub>2</sub> SCH <sub>2</sub> CH(CH <sub>3</sub> ) <sub>2</sub>	1.2	66
<b>13a</b>	CH <sub>2</sub> SCH <sub>2</sub> C <sub>6</sub> H <sub>5</sub>	51	NT
<b>14a</b>	CH <sub>2</sub> SCH <sub>2</sub> C <sub>6</sub> H <sub>11</sub>	74	> 100

<sup>a</sup> Values are means of two-three experiments (NT = not tested).

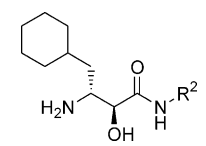


**Scheme 2.** Reagents and conditions: (a) Na, *i*-PrBr, NH<sub>3</sub>; (b) BOC<sub>2</sub>O, *i*-PrOH, H<sub>2</sub>O; (c) HN(OCH<sub>3</sub>)CH<sub>3</sub> HCl, EDCl, HOBT, NMM, CH<sub>2</sub>Cl<sub>2</sub>; (d) LiAlH<sub>4</sub>, Et<sub>2</sub>O; (e) TMSCN, ClCH<sub>2</sub>CH<sub>2</sub>Cl, 90 °C; (f) HCl, dioxane, H<sub>2</sub>O, 100 °C; (g) BOC<sub>2</sub>O, NMM, dioxane, H<sub>2</sub>O; (h) 3-chlorobenzoylhydrazide, EDCl, HOBT, NMM, CH<sub>2</sub>Cl<sub>2</sub>; (i) Diastereomer separation by HPLC (Silica, 20%acetone/hexanes); (j) HCl, dioxane.

N-terminal methionine and the relatively small active site opening observed in X-ray crystal structures of the enzyme, it was expected that large amide substituents would be poorly accommodated. While this seemed to hold for alkyl substituents (**6e–i**), aryl substituents were found to provide potent inhibitors (**6j–m**). Interestingly, a variety of linkers between the carbonyl and aryl moieties were accepted, including heteroatom linkers such as hydrazines and alkoxyamides (**6n–p**). Similar trends were seen for over 200 analogues of **2a** in a parallel study (results not shown).

To further explore these findings, a matrix synthesis was carried out combining side chains and carbonyl substituents (see Table 3 for monomer list). In this case a set of BOC-protected 3-amino-2-hydroxy acids<sup>12</sup> were activated as their HOBT esters using DCC resin in a mixture of DMA and dichloromethane for 5 min in 48 well blocks, followed by addition of the coupling

**Table 2.** Inhibition of human methionine aminopeptidases



Compd	NHR <sup>2</sup>	MetAP2 IC <sub>50</sub> , μM <sup>a</sup>	MetAP1 IC <sub>50</sub> , μM <sup>a</sup>
<b>6a</b>	L-AlaOEt	0.60	84
<b>6b</b>	D-AlaOEt	1.1	> 100
<b>6c</b>	HNC(CH <sub>3</sub> ) <sub>2</sub> CO <sub>2</sub> Et	0.97	> 100
<b>6d</b>	L-AlaOH	14	> 100
<b>6e</b>	L-LeuOMe	35	NT
<b>6f</b>	L-ValOMe	4.3	NT
<b>6g</b>	L-IleOMe	14	NT
<b>6h</b>	HNCH(CH <sub>3</sub> )CH(CH <sub>3</sub> ) <sub>2</sub>	> 100	NT
<b>6i</b>	HN(CH <sub>2</sub> ) <sub>6</sub> CH <sub>3</sub>	16	NT
<b>6j</b>	HNPh-3-OCH <sub>3</sub>	0.46	90
<b>6k</b>	HNCH <sub>2</sub> (2-Naphthyl)	0.16	12
<b>6l</b>	HNCH(CH <sub>3</sub> )(2-Naphthyl)	0.31	5.3
<b>6m</b>	HN(CH <sub>2</sub> ) <sub>2</sub> Ph-2,4-diCl	0.32	63
<b>6n</b>	HNNHC <sub>6</sub> H <sub>4</sub> -4-CH <sub>3</sub>	0.17	14
<b>6o</b>	HNOC <sub>6</sub> H <sub>5</sub>	0.20	20
<b>6p</b>	HNNHCOC <sub>6</sub> H <sub>3</sub> -2,5-diCl	0.29	> 100

<sup>a</sup> Values are means of two-three experiments (NT = not tested).

partners and agitation for 18 h. Following a quench with trisamine resin followed by isocyanate resin the mixtures were shaken for 4 h, filtered and washed with dichloromethane, then concentrated and purified by RPHPLC. Deprotection with 1:1 TFA/dichloromethane provided the test compounds, which were characterized by  $^1\text{H}$  NMR and MS and judged to have HPLC purity >90% prior to biological testing (see Table 3.)

The trends identified earlier among the  $\text{R}^1$  substituents generally were maintained, with groups approximating or slightly exceeding the volume of the methionine sidechain providing the best activity. Extended analogues providing the best activity. Extended analogues providing the best activity. The aromatic amides were generally superior in activity to the alanine containing counterparts, but the effects of the link and aromatic group on potency and selectivity showed dependence on  $\text{R}^1$  in a manner that was not immediately obvious. Crystallographic investigation of a series of enzyme–inhibitor complexes revealed that while the 3-amino-2-hydroxy amide portion of the inhibitors bound in a consistent manner across many structures, the portion of the inhibitors projecting out of the active site opening displayed considerable variation (see Fig. 1).<sup>13</sup> In particular, it was noted that the imidazole sidechain of His339 can adopt a number of conformations depending on the structure of the inhibitor. Use of a matrix synthesis was instrumental in optimizing this series in view of the variable binding modes that were observed.

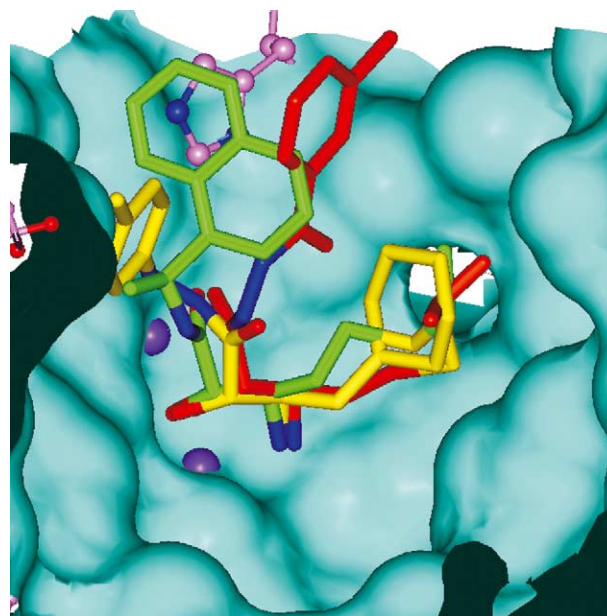
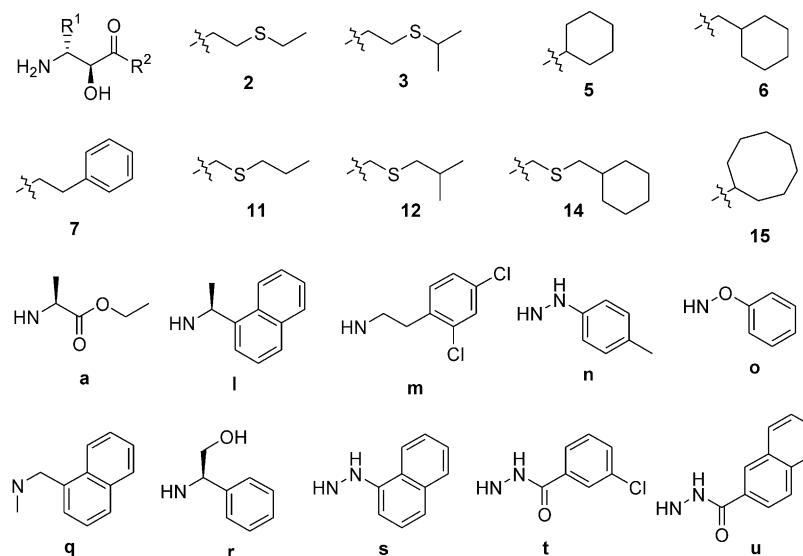


**Figure 1.** Overlaid MetAP2 complexes of **2l** (green), **3t** (red) and **6n** (yellow) from X-ray crystal structures of enzyme–inhibitor complexes. Residues forming the front of the active site were omitted for clarity. The active site  $\text{Mn}^{2+}$  atoms are shown as purple spheres. His339 is shown in lavender, in the conformation observed for the complex with **3t**.

**Table 3.** Enzyme inhibition assay results for matrix compounds<sup>a</sup>



	$\text{R}^2 = \text{a}$	<b>l</b>	<b>m</b>	<b>n</b>	<b>o</b>	<b>q</b>	<b>r</b>	<b>s</b>	<b>t</b>	<b>u</b>
$\text{R}^1 = \text{2}$	1.3/69	0.03/0.37	—	0.05/1.3	0.05/1.3	0.02/12	—	0.05/8.9	0.27/8.7	0.21/15
<b>3</b>	1.1/NT	0.19/12	0.48/69	0.05/11	0.05/4.7	0.13/81	0.25/32	—	<b>0.11/56</b>	0.25/18
<b>5</b>	13/NT	0.24/76	3.2/NT	4.9/NT	0.83/95	1.6/NT	0.9/79	1.0/89	0.9/46	51/NT
<b>6</b>	0.6/84	0.31/5.3	0.32/63	0.18/11	0.20/20	0.5/78	0.12/68	0.14/58	1.5/> 100	0.56/63
<b>7</b>	0.46/> 100	0.02/12	1.1/NT	0.80/16	0.31/13	0.19/> 100	0.42/75	0.50/93	2.7/NT	1.6/NT
<b>11</b>	1.4/57	0.04/1.6	0.62/24	0.43/5.0	0.05/1.7	1.0/NT	0.85/12	1.7/NT	0.29/11	—
<b>12</b>	1.2/66	0.05/2.2	0.27/53	0.06/6.8	0.03/1.5	0.12/19	0.14/11	0.12/34	0.13/8.1	0.07/NT
<b>14</b>	74/> 100	2.6/45	3.5/> 100	2.4/NT	3.6/NT	5.3/NT	—	8.6/NT	42/NT	—
<b>15</b>	—	—	1.3/NT	2.1/NT	0.7/> 100	4.1/NT	1.5/NT	6.1/NT	1.2/NT	—

<sup>a</sup> Values reported are  $\text{IC}_{50}$  for MetAP2/MetAP1, and are means of two–three experiments (NT = not tested, — = compound not prepared).

Among the compounds in Table 3, **3t** (A-357300) was of particular interest, and a larger scale synthesis was achieved by the route shown in Scheme 2.<sup>12b</sup> The X-ray crystal structure of the enzyme–inhibitor complex of **3t** (Fig. 1) indicates the mode of binding. The 2-hydroxy-3-aminoamide grouping interacts with the active site Mn<sup>2+</sup> metal ions,<sup>11</sup> with the 2-hydroxy substituent bridging between them. The thioether-containing side-chain largely fills the adjacent hydrophobic site, while the 3-chlorophenyl aromatic group lies face to face with the histidine-339 imidazole. Both hydrophobic groups interact near the site of an insertion<sup>1</sup> absent in MetAP1.

In addition to good potency and selectivity against the isolated enzymes, compound A-357300 proved to be a potent inhibitor of HMVEC (human microvascular endothelial cell) proliferation, displaying an IC<sub>50</sub> of 100 nM,<sup>14</sup> and of cellular MetAP2 activity in HMVEC.<sup>15</sup> Further biological characterization of this compound and its examination in in vivo models of angiogenesis and cancer has been recently described.<sup>15</sup>

In this study, the combined use of a structure-based approach with high throughput parallel synthesis and directed matrix combinatorial synthesis allowed optimization of the initial lead structure. Improvements to the potency, selectivity and other properties provided a reversible inhibitor of MetAP2 suitable for evaluation of this approach to inhibition of angiogenesis and tumor growth.

#### References and notes

- Arfin, S. M.; Kendall, R. L.; Hall, L.; Weaver, L. H.; Stewart, A. E.; Matthews, B. W.; Bradshaw, R. A. *Proc. Natl. Acad. Sci. U.S.A.* **1995**, *92*, 7714.
- Sin, N.; Meng, L.; Wang, M. Q.; Wen, J. J.; Bornmann, W. G.; Crews, C. M. *Proc. Natl. Acad. Sci. U.S.A.* **1997**, *94*, 6099.
- Griffith, E. C.; Su, Z.; Turk, B. E.; Chen, S.; Chang, Y. H.; Wu, Z.; Biemann, K.; Liu, J. O. *Chem. Biol.* **1997**, *4*, 461.
- Liu, S.; Widom, J.; Kemp, C. W.; Crews, C. M.; Clardy, J. *Science* **1998**, *282*, 1324.
- Ingber, D. In *Cancer Therapeutics*; Teicher, B. A., Ed.; Humana Press: Totowa, NJ, 1997; p 283.
- Umezawa, H.; Aoyagi, T.; Suda, H.; Hamada, M.; Takeuchi, T. *J. Antibiot.* **1976**, *29*, 97.
- Aoyagi, T.; Tobe, H.; Kojima, F.; Hamada, M.; Takeuchi, T.; Umezawa, H. *J. Antibiot.* **1978**, *31*, 636.
- Keding, S. J.; Rich, D. H. In *Peptides for the New Millennium*; Fields, G. B., Tam, J. P., Barany, G., Eds.; Kluwer Academic Publishers: Dordrecht/Boston/London, 2000; p 431.
- Marino, J. P., Jr.; Ryan, M. D.; Thompson, S. K.; Veber, D. F. PCT International Publication Number WO 01/36404.
- Nishizawa, R.; Saino, T.; Takita, T.; Suda, H.; Aoyagi, T.; Umezawa, H. *J. Med. Chem.* **1977**, *20*, 510.
- Wang, J.; Sheppard, G. S.; Lou, P.; Kawai, M.; Park, C.; Egan, D. A.; Schneider, A.; Bouska, J.; Lesniewski, R.; Henkin, J. *Biochemistry* **2003**, *42*, 5035. A coupled-enzyme chromogenic assay was used to measure methionine aminopeptidase activity by monitoring production of free methionine with L-amino acid oxidase and horseradish peroxidase. Compounds in 10 mM DMSO stock solutions were serially diluted with 50 mM Hepes buffer pH 7.4 containing 150 mM NaCl and the solutions added to an enzyme–substrate mixture containing MetAP2 or MetAP1, MAS peptide, coupling enzymes and substrate. A450 was recorded every 20 seconds for 20 min at room temperature.
- (a) Syntheses described in: Craig, R. A.; Henkin, J.; Kawai, M.; Lynch, L. L.; Patel, J.; Sheppard, G. S.; Wang, J. U.S. Patent 6,242,494, June 5, 2001. (b) Craig, R. A.; Kawai, M.; Lynch, L. M.; Patel, J. R.; Sheppard, G. S.; Wang, J.; Yang, F.; BaMaung, N. Y. PCT International Publication Number WO 01/79157; U.S. Patent Application US2002002152.
- Refined crystallographic coordinates for the structures of MetAP2 complexed with ligands **2l**, **3t** and **6n** have been deposited with the Protein Data Bank ([www.rcsb.org](http://www.rcsb.org)) with entry codes 1R58, 1R5G and 1R5H.
- HMVEC proliferation was measured using MTS reagents after a period of 3 days in complete growth medium EGM2 containing a combination of growth factors (VEGF, bFGF, EGF, IGF) and FBS: Wang, J.; Lou, P.; Henkin, J. *Biochemistry* **2000**, *77*, 465.
- Wang, J.; Sheppard, G. S.; Lou, P.; Kawai, M.; BaMaung, N. Y.; Erickson, S. A.; Tucker-Garcia, L.; Park, C.; Bouska, J.; Wang, Y.-C.; Frost, D.; Tapang, P.; Albert, D.; Morgan, S.; Morowitz, M.; Shusterman, S.; Maris, J. M.; Lesniewski, R.; Henkin, J. *Cancer Research* **2003**, *63*, 7861.